ACS Photonics

Letter

pubs.acs.org/journal/apchd5

Metal–Dielectric Waveguides for High-Efficiency Coupled Emission

Ramachandram Badugu,[†] Henryk Szmacinski,[†] Krishanu Ray,[†] Emiliano Descrovi,[‡] Serena Ricciardi,[‡] Douguo Zhang,[§] Junxue Chen,[∥] Yiping Huo,[⊥] and Joseph R. Lakowicz*,[†]

[†]Center for Fluorescence Spectroscopy, Department of Biochemistry and Molecular Biology, University of Maryland School of Medicine, 725 W. Lombard Street, Baltimore, Maryland 21201, United States

[‡]Department of Applied Science and Technology, Polytechnic University of Turin, Corso Duca degli Abruzzi 24, 10129 Turin, Italy

[§]Institute of Photonics, Department of Optics and Optical Engineering, University of Science and Technology of China, Hefei, Anhui 230026, China

[∥]School of Science, Southwest University of Science and Technology, Mianyang, Sichuan 621010, China

[⊥]School of Physics and Information Technology, Shaanxi Normal University, Xi'an 710062, China

Supporting Information

ABSTRACT: We report a metal–dielectric planar structure that provides high-efficiency coupling of fluorescence at distances over 100 nm away from the metal surface. This hybrid metal–dielectric waveguide (MDW) consists of a continuous metal film coated with a dielectric layer. We observed efficient long-range coupling of rhodamine B on top of a 130 nm layer of silica, resulting in a narrow angular distribution of the emission. The high-efficiency radiation through the Ag film appears to be due to coupling of the fluorophore to an optical waveguide mode with a long propagation length and a narrow resonance. The results were consistent with simulations. These multilayer structures can be made using vapor deposition and/or spin coating, and the silica surface can be used for conjugation to biomolecules and surface-selective detection. This simple hybrid metal–dielectric structure provides new opportunities for fluorescence sensing, genomics, proteomics, and diagnostics.

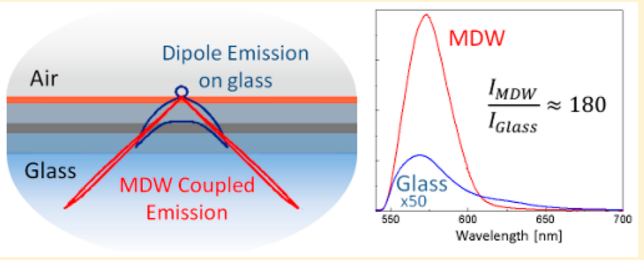

KEYWORDS: *metal–dielectric waveguide, waveguide-coupled emission, plasmon-controlled fluorescence, surface plasmon-coupled emission, surface plasmon-enhanced fluorescence, total internal reflection*

For the past decade, there has been extensive research using metallic surfaces and particles to modify the decay times and spatial distributions of fluorescence.[1−5] This control of emission is made possible by the near-field interactions of fluorophores (dipoles) with plasmons on the metal structures.[6−8] These near-field interactions allow the radiation rates and spatial radiation patterns of the dipoles to be modified by the optical properties of the metallic structures. Many of these structures contain nanoscale features that are made using top-down nanofabrication. This approach is costly for large areas, which in turn has limited their uses in biomedical research. Useful control of fluorescence can also be accomplished with continuous thin metal films. Fluorophores within about 50 nm from the metal surface can radiate light through the metal film, resulting in a cone of emission over a narrow angular range, exiting the bottom of the metal-coated glass slide and prism.[9,10] This phenomenon is called surface plasmon-coupled emission (SPCE). Theoretical[11,12] and experimental[9,10] studies of surface plasmon-coupled emission have shown that fluorophores within about 10 nm of the metal are quenched. Hence surface plasmon-coupled emission occurs for fluorophores in a region 10 to 50 nm above the metal. The emission from more distant fluorophores is reflected by the metal, which decreases the emission contribution of the bulk region of the sample to the coupled emission. The quenching at short distances can decrease sensitivity of detecting surface-bound fluorophores. The sensitivity is also decreased because some fraction of the emission escapes detection by radiation into free space above the structure.

In this paper we report a simple multilayer structure that displays efficient coupling through the metal film with only a small fraction of the emission appearing in the free-space direction. This metal–dielectric waveguide (MDW) structure consists of a continuous thin metal film coated with a fractional wavelength thickness of a dielectric, in the present case being Ag and silica films, respectively. Fluorophores on top of the silica, over 100 nm from the metal surface, couple radiation into the waveguide modes of the structure, resulting in a waveguide-coupled emission (WCE). The waveguide-coupled emission occurs over a narrow angular range, which is determined by the dispersion of the optical modes sustained by the structure. This observation is distinct from previous reports of waveguide

Received: April 25, 2015
Published: June 26, 2015

 © 2015 American Chemical Society

DOI: 10.1021/acsphotonics.5b00219
ACS Photonics 2015, 2, 810–815

surface plasmon-coupled emission, where the fluorophores were present throughout the dielectric layer[13,14] and a significant fraction of the fluorophores were within 50 nm of the metal surface. In the present study, the probes are distant from the metal and couple over a distance greater than 100 nm from the metal film. Our results are different from surface plasmon-enhanced fluorescence (SPEF), which uses the plasmon-enhanced field for excitation but only the free-space emission is observed.[15,16] Also our findings are different from the observed directional emission using planar dielectric antennas reported previously.[17] The metal−dielectric waveguide used in this report displays efficient coupled emission from fluorophores on the surface of the structure with the emission emerging from the bottom of the substrate. The efficient coupling of surface-bound fluorophores is convenient for bioassays. More generally, hybrid metal−dielectric multilayers display both waveguide and plasmonic modes, resulting in both S- and P-polarized emission, respectively, which may be useful for resolving different populations or orientations of biomolecules.

RESULTS AND DISCUSSION

Metal films coated with a dielectric layer are known to display waveguide modes.[16] Illumination at appropriate wavelengths and angles results in field intensity distributions within the dielectric layer corresponding to the illuminated mode. Previous reports showed that fluorophores within the dielectric layer could couple with the optical modes to obtain surface plasmon-coupled emission.[12−14] We questioned if fluorophores on top of the dielectric layer, as shown schematically in Figure 1, could also couple with the modes sustained by the structure

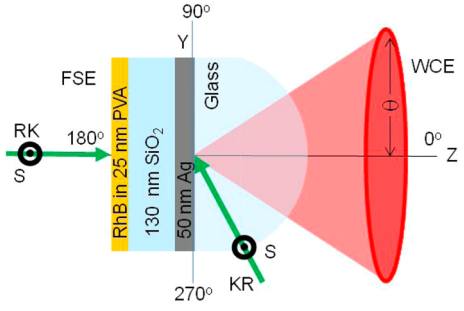

Figure 1. Optical configuration for measurements with the MDW.

and result in coupled emission. We found no reports of fluorophore coupling from this location, which is distant from the metal surface. Excitation of the metal−dielectric waveguide structure can be accomplished through the underlying prism, which is called the Kretschmann (KR) configuration, and from the air or sample side, which is called the reverse Kretschmann (RK) configuration. We proceeded with experiments using a range of silica thicknesses to determine the distances over which coupled emission could occur. Using the KR geometry and P-polarized excitation we examined the emission from rhodamine B (RhB) embedded in a poly(vinyl alcohol) (PVA) layer on top of the metal−dielectric structure, with various thicknesses of silica. As expected, we found a decrease in the P-polarized surface plasmon-coupled emission intensity as the silica thickness was increased from 0 to about 80 nm (data not shown).[11] However, for silica thicknesses near 100 nm with S-polarized illumination we observed an increase in the S-polarized coupled emission (SCE) intensity (Figure 2). Unless

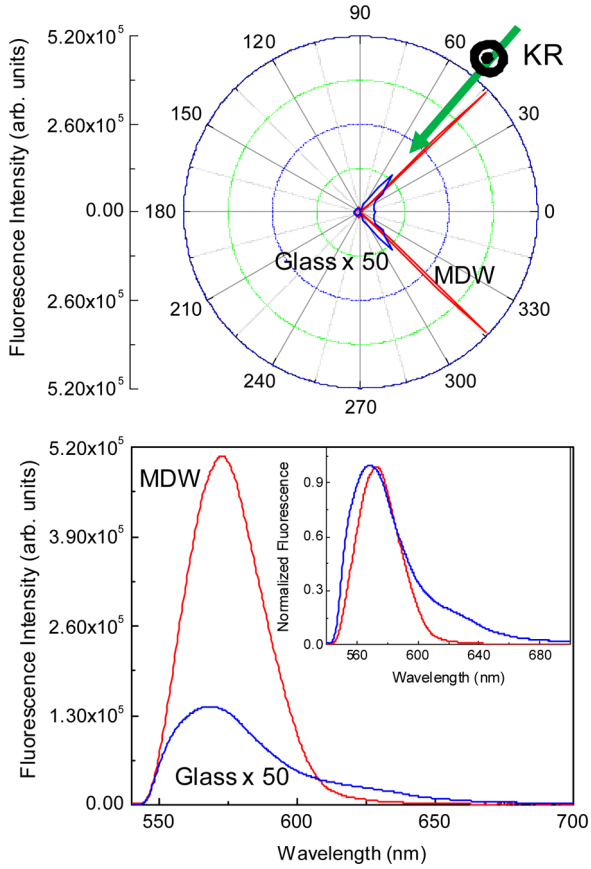

Figure 2. Angular emission distributions for RhB on the MDW (red) and glass slide (blue) (top). Emission spectra of RhB on the MDW and glass slide (bottom). Inset figure in the bottom panel shows the corresponding normalized emission spectra. The angle-dependent emission intensity on glass (top) and emission spectra from glass are multiplied by 50 to visualize. Excitation using an S-polarized 532 nm CW laser at 49 degrees (KR).

stated otherwise, all subsequent measurements refer to S-polarized incidence and observation. For a silica thickness of 130 nm we observed strong RhB emission coupled through the structure, with a very narrow angular distribution near ∼44° from the normal (Figure 2, top). The angular emission distribution was narrower than we observed for probes immediately adjacent to the Ag film.[9,10] Additionally, at this collection angle, the detected intensity is 180-fold higher than found for RhB on a glass slide (Figure 2, bottom). Importantly, a significant fraction of the overall emission is coupled through the structure, and little free-space emission was observed.

The results in Figure 2 were obtained with excitation in Kretschmann configuration, which is S-polarized 532 nm light incident through the prism at 49 degrees. This is the incidence angle that yielded the highest coupled emission intensities. Similar results were also found with reverse Kretschmann excitation, wherein the excitation is at normal incidence from the air, upper space (180 deg). At this angle the S and P designations do not apply. The incident polarization was parallel to the S-polarized observation. A higher free-space emission is observed with RK excitation, which can be explained by excitation of the entire thickness of PVA (Figure S1). For both KR and RK excitation, the coupled emission was found to be almost completely S-polarized and highly directional. At a 44 degree collection angle, the fluorescence

DOI: 10.1021/acsphotonics.5b00219
ACS Photonics 2015, 2, 810−815

radiation emitted from the metal−dielectric waveguide sample with RK excitation still shows a higher intensity as compared to the glass sample. However, such an increase of intensity is significantly smaller with the excitation using an RK configuration (20-fold) as compared to that with the KR excitation (180-fold).

Before discussing the role of excitation in the emission enhancement effect, it is useful to examine the angular and spectral distribution of the coupled radiation. We measured emission spectra at angles offset from the angle with maximum emission intensity (44 degrees). In the KR configuration, the intensity of the coupled radiation was found to decrease 2-fold or more with an angular change of 1°, and the emission is close to zero with a 3° offset (Figure 3). An analogous behavior was

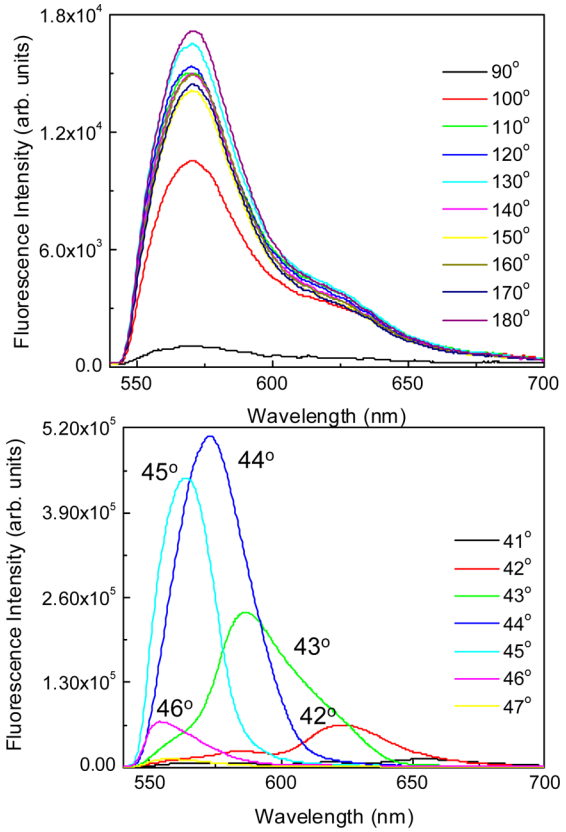

Figure 3. Angle-dependent emission spectra of RhB on the surface of the MDW shown in Figure 1. KR excitation using an S-polarized 532 nm CW laser. The incident angle is 49 degrees.

found for RK excitation (Figure S2). In addition to the decreased intensity, the collected emission spectra show a shift of the maximum peak as a function of the observation angle (Figures 3 and S2). In contrast, the free-space emission did not display any significant spectral shifts or intensity variations with changes in the observation angle. The experimental observations reported so far suggest that two separate mechanisms are involved in the high-intensity directional emission observed with the metal−dielectric waveguide structure. A first mechanism is the coupling of power radiated from excited emitters in the PVA layer into the optical mode sustained by the multilayer. A second mechanism is the enhanced excitation of emitters by means of the resonant coupling of the incident laser beam to the optical mode sustained by the metal−dielectric waveguide structure.

The mode coupling of emitted radiation has been addressed by using a simple computational model for planar structures.[18] A 25 nm thick PVA layer homogeneously covers a metal−dielectric waveguide structure constituted by a 50 nm thick silver layer on a glass substrate and a 130 nm thick silica layer. This multilayer structure is sandwiched between an upper and lower half-space made of air and glass, respectively. In this simulation the PVA layer hosts a 1 nm thick emitter layer, which can be located at several distances from the PVA top surface. In the following, the emitter layer will be at 1 nm from the PVA top surface. The emitter layer possesses a homogeneous dipole momentum oriented perpendicularly to the scattering plane, perpendicular to the plane of Figure 1. In this way, the main part of the radiated power observed at any collection angle in the scattering plane will be S-polarized. Finally, for comparison purposes, an identical arrangement for the silica layer, PVA layer, and the emitter layer is considered on a bare glass substrate. As wavelengths from 550 to 620 nm are considered in the computation, an overall intensity integrated over this spectral range is calculated and plotted in the polar diagram shown in Figure 4. The fluorescence

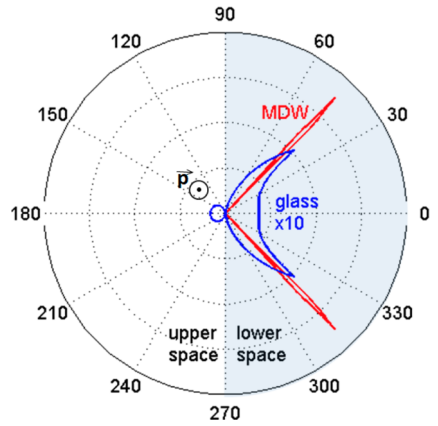

Figure 4. Calculated angular emission distribution for an emitter layer located within a 25 nm thick PVA layer on either the MDW structure (red line) or a bare glass substrate (blue line). Radiated power is integrated over the spectral range from 550 to 620 nm. The emitter has a dipole (D) momentum perpendicular to the observation plane, as indicated in the figure, and is located in a 1 nm layer of PVA that is 1 nm below the top of the PVA. The lower space is constituted by a semi-infinite glass substrate, while the upper space is air.

emission in the metal−dielectric waveguide structure is found to be highly directional into the glass substrate, wherein 82% of the overall radiated power leaks at angles symmetrically offset by 44 degrees from the normal. The calculated emission intensity is about 20-fold higher for the metal−dielectric waveguide structure as compared to the bare glass substrate, thus confirming quantitatively the experimental findings.

The directional emission observed on planar multilayers is due to the coupling of the radiated power into the modes sustained by the structures. Modes in planar multilayers can be calculated by using well-known methods based on the transfer matrix. In our case, we calculated the angularly resolved spectral reflectivity of the metal−dielectric waveguide structure upon S-polarized illumination from the glass substrate (Figure 5). In order to take into account losses (absorption and scattering due to surface roughness), the following complex refractive indexes are used: $n_{silica} = 1.46 + 4i \times 10^{-4}$, $n_{PVA} = 1.48+i \times 10^{-3}$ for

DOI: 10.1021/acsphotonics.5b00219
ACS Photonics 2015, 2, 810−815

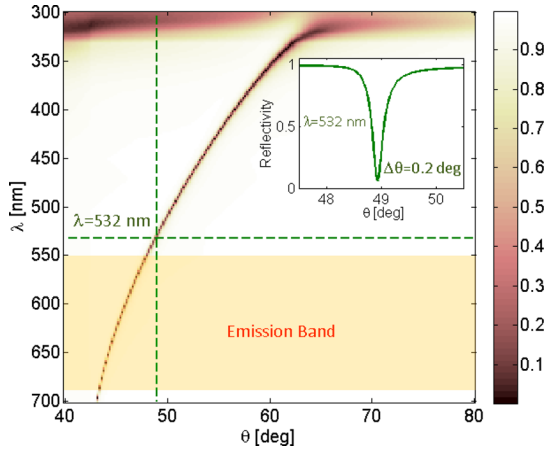

Figure 5. Angularly resolved spectral reflectivity for S-polarized light illuminating the metal−dielectric waveguide from the glass substrate. The dark, low-reflectivity region indicates the waveguide mode dispersion. At a wavelength λ = 532 nm, the mode resonance is centered at θ = 49 degrees and has an angular width $\Delta\theta$ = 0.2 degree (inset).

silica and PVA, respectively. The optical constants for silver in the spectral range from 550 nm to 620 are taken according to published values.[10] An S-polarized waveguide mode is found as a narrow reflectivity dip dispersed at angles larger than the critical angle for a glass/air interface. As a clear evidence of the mode-coupled nature of the observed fluorescence reported above, the angle-dependent emission maxima in Figure 3 were found to agree with the calculated mode dispersion.

The excitation of this waveguide mode by an incident laser radiation is responsible for the additional increase of the coupled emission intensity as observed in Figure 2. As shown in Figure 5, it is possible to couple far-field, S-polarized radiation at λ = 532 nm into the metal−dielectric waveguide mode, provided an incidence angle θ = 49 degrees. The electric field $|E|^2$ distribution across the metal−dielectric waveguide obtained at such illumination condition is shown in Figure 6a. The asymmetry of the planar waveguide structure makes the mode profile asymmetrically peaked toward the PVA layer, resulting in about 120-fold field intensity on the PVA surface. In contrast, the field intensity on a PVA-coated glass slide, for the same illumination condition, is enhanced only by 4-fold, as expected for total internal reflection (TIR). It is well known that the evanescent fields above the gold or silver films used for surface plasmon resonance are limited to enhancements near 50-fold.[19−21] The higher fields obtained in the metal−dielctric waveguide is due to the field being displaced away from the lossy metal toward the top of the dielectric, resulting in a narrower resonance and a correspondingly higher Q factor. A similar case is represented by Bloch surface waves, which are optical modes bound at the surface of dielectric multilayers.[22−24]

The resonant excitation of RhB with mode coupling of the illumination laser and the directional emission represent two independent mechanisms summing up their effects when occurring simultaneously. Therefore, the 120-fold excitation enhancement and the 20-fold emission enhancement discussed above should provide an overall 600-fold enhancement in the intensity collected at about 44 degrees in the KR configuration, as compared to a bare glass substrate (taking advantage of a 4-fold excitation enhancement due to TIR). However, as shown

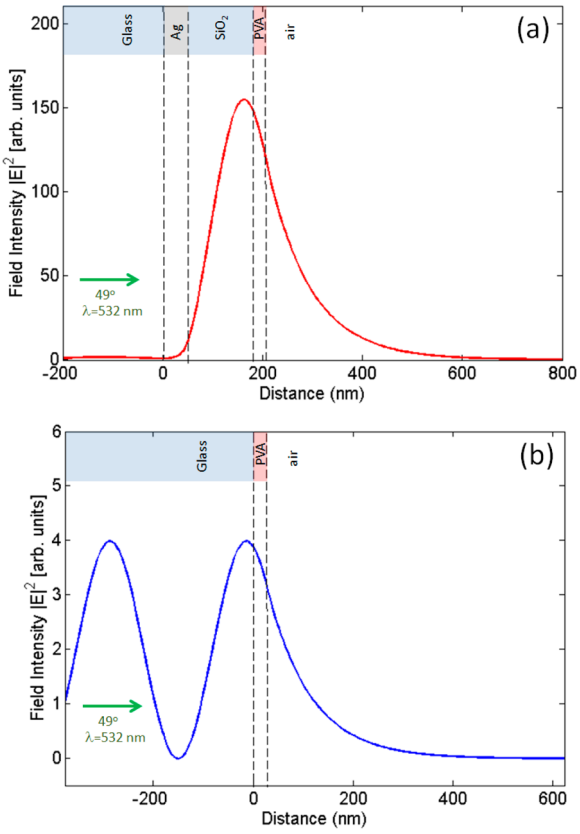

Figure 6. Electric field intensities for 532 nm light incident on the MDW (a) and glass (b). Note the 30-fold difference in the field intensity in the PVA layer.

in Figure 2, only a 180-fold enhancement was observed when comparing the fluorescence intensity collected from the MDW structure and the bare glass substrate in KR. We believe this discrepancy is caused by a nonoptimal coupling of the metal−dielectric waveguide mode from the illumination laser beam. An optimal resonant coupling would require an illumination beam divergence comparable to the angular width of the mode to be coupled in ref 25. As the MDW mode we are considering is characterized by an angularly narrow resonance ($\Delta\theta$ = 0.2 degree), the laser could not exhibit a correspondingly low divergence, resulting in a field enhancement in the PVA layer lower than expected.

CONCLUSION

We described a simple multilayer structure that acts as a hybrid waveguide sustaining a guided mode between the dielectric and metal surfaces. For a given combination of dielectric thickness and emission wavelength, fluorophores on top of the structure efficiently couple into the S-polarized optical mode and radiate most of the energy through the metal film on the glass substrate. The high intensity of the coupled emission is due to a combination of effects including an increased excitation field and efficient redirection of emitted power. In contrast to the structures used for surface palasmon-coupled emission, metal−dielectric waveguide substrates provide high enhanced emission. This is due to minimized metal quenching effect in the metal−dielectric waveguide substrates with the probes located away from the lossy metal surface. Also, as stated earlier, due to the asymmetry of the planar waveguide structure, the waveguide mode profile is asymmetrically peaked toward

DOI: 10.1021/acsphotonics.5b00219
ACS Photonics 2015, 2, 810−815

the PVA layer, resulting in about 120-fold field intensity on the PVA surface. Similar fields above the gold or silver films used for surface plasmon resonance or surface plasmon-coupled emission are limited to near 50-fold. Experimentally, we observed over 100-fold higher coupled emission intensity from the metal−dielectric waveguide used in the present study as compared to the structure used for surface plasmon-coupled emission, where the thickness of silica is 3 nm (data not shown). This simple multilayer design can be readily modified for different absorption and/or emission wavelengths by changes in dielectric layer thickness and/or a different metal film. The multilayer format offers opportunities for advanced approaches to high-throughput arrays or clinical diagnostics.

MATERIALS AND METHODS

The metal−dielectric waveguide substrates were made using magnetron sputtering (Hummer 6.6 RF, Anatech USA) of Ag and SiO_2 layers on precleaned standard microscope glass slides. The sample was subsequently coated with RhB-doped PVA in water, 0.5% PVA (MW 16 000−23 000), 3000 rpm for 1 min,[13,14] which yielded a thickness of 25 nm. The thicknesses of the Ag, silica, and PVA layers were confirmed using an N&K spectroscopic ellipsometer.

The angular-dependent emission measurements were performed using the optical configuration shown in Figure 1. The structure is placed on a cylindrical prism with a refractive index matching fluid, glycerol. Excitation was with a CW 532 nm Nd-YVO_4 laser with polarizer between the laser and sample. The emission was collected with a 1 mm diameter fiber positioned 2 cm from the sample, leading to an estimated angular resolution of 1.4 degrees. Emission spectra were measured using a model SD2000 Ocean Optics spectrometer with 1 nm intervals. A 550 nm long-pass emission filter and a polarizer were also placed between the sample and fiber input to remove scattered light at 532 nm. Two modes of excitation are possible. Excitation through the prism is called the Kretschmann configuration. Excitation from the free-space direction is called reverse Kretschmann. Emission coupled thorough the structure and observed through the prism is called waveguide coupled emission. Emission away from the top of the MDW is called free-space emission. S-polarization has the electric field parallel to the surface and perpendicular to the incidence plane. P-polarization has the electric field contained in the incidence plane. The electrical field component perpendicular to the surface is dependent on incident angle. Unless stated otherwise, all emission intensities and spectra were measured with an S-oriented polarizer.

Simulations of the optical properties of the MDWs were performed using two software packages with consistent results. The field intensities due to incident light were calculated using TFCalc from Software Spectra, Inc. and by independent code written by one of the authors (E.D.).[15]

ASSOCIATED CONTENT

Supporting Information

The data obtained using RK illumination are included in the Supporting Information. Figures S1 describes angular emission distributions and emission spectra of RhB on the MDW and glass slide. Figure S2 presents the angle-dependent emission spectra of RhB on the surface of the MDW. The Supporting Information is available free of charge on the ACS Publications website at DOI: 10.1021/acsphotonics.5b00219.

AUTHOR INFORMATION

Corresponding Author

*E-mail: jlakowicz@som.umaryland.edu.

Notes

The authors declare no competing financial interest.

ACKNOWLEDGMENTS

This work was supported by grants to J.R.L. from the National Institute of Health, GM107986, EB006521, and OD019975. This work was also supported by the National Key Basic Research Program of China under grant no. 2013CBA01703 and the National Natural Science Foundation of China under grant nos. 61427818, 11374286, and 11204251.

REFERENCES

(1) Rui, G.; Zhan, Q. Highly sensitive beam steering with plasmonic antenna. *Sci. Rep.* **2014**, *4*, 5962−1−5.
(2) Aouani, H.; Mahboub, O.; Bonod, N.; Devaux, E.; Popov, E.; Rigneault, H.; Ebbesen, T. W.; Wenger, J. Bright unidirectional fluorescence emission of molecules in a nanoaperture with plasmonic corrugations. *Nano Lett.* **2011**, *11*, 637−644.
(3) Aouani, H.; Mahboub, O.; Devaux, E.; Rigneault, H.; Ebbesen, T. W.; Wenger, J. Plasmonic antennas for directional sorting of fluorescence emission. *Nano Lett.* **2011**, *11*, 2400−2406.
(4) Lakowicz, J. R.; Ray, K.; Chowdhury, M.; Szmacinski, H.; Fu, Y.; Zhang, J.; Nowaczyk, K. Plasmon-controlled fluorescence: a new paradigm in fluorescence spectroscopy. *Analyst* **2008**, *133*, 1308−1346.
(5) Cao, S.-H.; Cai, W.-P.; Liu, Q.; Li, Y.-Q. Surface plasmon-coupled emission: What can directional fluorescence bring to the analytical sciences? *Annu. Rev. Anal. Chem.* **2012**, *5*, 317−336.
(6) Mertens, H.; Koenderink, A. F.; Polman, A. Plasmon-enhanced luminescence near noble-metal nanospheres: Comparison of exact theory and an improved Gersten and Nitzan model. *Phys. Rev. B: Condens. Matter Mater. Phys.* **2007**, *76*, 115123−1/2.
(7) Carminati, R.; Greffet, J.-J.; Henkel, C.; Vigoureux, J. M. Radiative and non-radiative decay of a single molecule close to a metallic nanoparticle. *Opt. Commun.* **2006**, *261*, 368−375.
(8) Lakowicz, J. R. Radiative decay engineering 5: metal-enhanced fluorescence and plasmon emission. *Anal. Biochem.* **2005**, *337*, 171−194.
(9) Lakowicz, J. R. Radiative decay engineering 3. Surface plasmon-coupled directional emission. *Anal. Biochem.* **2004**, *324*, 153−169.
(10) Gryczynski, I.; Malicka, J.; Gryczynski, Z.; Lakowicz, J. R. Radiative decay engineering 4. Experimental studies of surface plasmon-coupled directional emission. *Anal. Biochem.* **2004**, *324*, 170−182.
(11) Enderlein, J.; Ruckstuhl, T. The efficiency of surface-plasmon coupled emission for sensitive fluorescence detection. *Opt. Express* **2005**, *13*, 8855−8865.
(12) Calander, N. Surface plasmon-coupled emission and Fabry-Perot resonance in the sample layer: A theoretical approach. *J. Phys. Chem. B* **2005**, *109*, 13957−13963.
(13) Gryczynski, I.; Malicka, J.; Nowaczyk, K.; Grycyznski, Z.; Lakowicz, J. R. Waveguide-modulated surface plasmon-coupled emission of Nile blue in poly(vinyl alcohol) thin films. *Thin Solid Films* **2006**, *510*, 15−20.
(14) Gryczynski, I.; Malicka, J.; Nowaczyk, K.; Gryczynski, Z.; Lakowicz, J. R. Effects of sample thickness on the optical properties of surface plasmon-coupled emission. *J. Phys. Chem. B* **2004**, *108*, 12073−12083.
(15) Li, L.; Granet, G.; Plumey, J. P.; Chandezon, J. Some topics in extending the C method to multilayer gratings of different profiles. *Pure Appl. Opt.* **1996**, *5*, 141−156.
(16) Saleh, B. E. A.; Teich, M. C. *Fundamentals of Photonics*; Wiley-Interscience, 2007; p 1177.

DOI: 10.1021/acsphotonics.5b00219
ACS Photonics 2015, 2, 810−815

(17) Lee, K. G.; Chen, X. W.; Eghlidi, H.; Kukura, P.; Lettow, R.; Renn, A.; Sandoghdar, V.; Götzinger, S. A planar dielectric antenna for directional single-photon emission and near-unity collection efficiency. *Nat. Photonics* **2011**, *5*, 166−169.
(18) Polerecký, L.; Hamrle, J.; MacCraith, B. D. Theory of the radiation of dipoles placed within a multilayer system. *Appl. Opt.* **2000**, *39* (22), 3968−3977.
(19) Dostalek, J.; Knoll, W. Biosensors based on surface plasmon-enhanced fluorescence spectroscopy. *Biointerphases* **2008**, *3*, FD12−FD22.
(20) Touahir, L.; Tobias, A.; Jenkins, A.; Boukherroub, R.; Gouget-Laemmel, A. C.; Chazalviel, J.-N.; Peretti, J.; Ozanam, F.; Szunerits, S. Surface plasmon-enhanced fluorescence spectroscopy on silver based SPR substrates. *J. Phys. Chem. C* **2010**, *114*, 22582−22589.
(21) Homola, J. Present and future of surface plasmon resonance biosensors. *Anal. Bioanal. Chem.* **2003**, *377*, 528−539.
(22) Meade, R. D.; Brommer, K. D.; Rappe, A. M.; Joannopoulos, J. D. Electromagnetic Bloch waves at the surface of a photonic crystal. *Phys. Rev. B: Condens. Matter Mater. Phys.* **1991**, *44*, 10961−10964.
(23) Ballarini, M.; Frascella, F.; Michelotti, F.; Digregorio, G.; Rivolo, P.; Paeder, V.; Musi, V.; Giorgis, F.; Descrovi, E. Bloch surface waves-controlled emission of organic dyes grafted on a one-dimensional photonic crystal. *Appl. Phys. Lett.* **2011**, *99*, 043302.
(24) Ditlbacher, H.; Krenn, J. R.; Felidj, N.; Lamprecht, B.; Schider, G.; Salerno, M.; Leitner, A.; Aussenegg, F. R. Fluorescence imaging of surface plasmon fields. *Appl. Phys. Lett.* **2002**, *80*, 404−406.
(25) Ulrich, R. Theory of the prism-film coupler by plane wave analysis. *J. Opt. Soc. Am.* **1970**, *60*, 1337−1350.

DOI: 10.1021/acsphotonics.5b00219
ACS Photonics 2015, 2, 810−815